

FRAME-VOYAGER: LEARNING TO QUERY FRAMES FOR VIDEO LARGE LANGUAGE MODELS

Anonymous authors

Paper under double-blind review

ABSTRACT

Video Large Language Models (Video-LLMs) have made remarkable progress in video understanding tasks. However, they are constrained by the maximum length of input tokens, making it impractical to input entire videos. Existing frame selection approaches, such as uniform frame sampling and text-frame retrieval, fail to account for the information density variations in the videos or the complex instructions in the tasks, leading to sub-optimal performance. In this paper, we propose FRAME-VOYAGER that learns to query informative frame combinations, based on the given textual queries in the task. To train FRAME-VOYAGER, we introduce a new data collection and labeling pipeline, by ranking frame combinations using a pre-trained Video-LLM. Given a video of M frames, we traverse its T -frame combinations, feed them into a Video-LLM, and rank them based on Video-LLM’s prediction losses. Using this ranking as supervision, we train FRAME-VOYAGER to query the frame combinations with lower losses. In experiments, we evaluate FRAME-VOYAGER on four Video Question Answering benchmarks by plugging it into two different Video-LLMs. The experimental results demonstrate that FRAME-VOYAGER achieves impressive results in all settings, highlighting its potential as a plug-and-play solution for Video-LLMs. The source code and the generated data will be open-sourced.

1 INTRODUCTION

Recent studies (Liu et al., 2023; 2024a; Li et al., 2024c; Lin et al., 2024b) explore integrating Large Language Models (LLMs, Stiennon et al. (2020); Gao et al. (2023); OpenAI (2023); Touvron et al. (2023); Jiang et al. (2023); Yang et al. (2024)) with visual foundation models (*e.g.*, Vision Transformer (ViT, Dosovitskiy et al. (2021)) and cross-modal projectors (Li et al., 2023a; Lin et al., 2024a; Liu et al., 2023)). In this paper, we focus on Video-LLMs. Existing Video-LLMs (Zhang et al., 2023; Cheng et al., 2024; Li et al., 2024b) usually treat the video as a sequence of image frames. The key challenge is that the entire video can not be fed into the model due to LLMs’ token length limitation (Xue et al., 2024). Meanwhile, arbitrarily increasing the token length of the model (Miao et al., 2023; Wan et al., 2024; Xiong et al., 2024; Zhang et al., 2024a) may lead to the “lost-in-the-middle” issue (Liu et al., 2024c) and introduce significant computational complexity.

To mitigate this issue, some efforts propose to select only a subset of frames as input, *e.g.*, through uniform sampling (Liu et al., 2023; Lin et al., 2024b; Cheng et al., 2024) or text-frame matching (Liang et al., 2024; Wang et al., 2024a; Yu et al., 2024). The uniform sampling strategy evenly samples frames in videos, while text-frame matching typically retrieves a set of relevant frames by calculating semantic similarities, *e.g.*, using CLIP (Radford et al., 2021), between the query and each frame. However, the uniform sampling fails to account for the information density variations in the videos. For instance, in the video question answering task, answering different questions may rely on distinct video segments or frames (Fu et al., 2024a). Meanwhile, text-frame matching is inadequate for complex video understanding tasks that require multi-frame or temporal reasoning, such as tracking the progression of an action or understanding cause-and-effect relationships over time. For instance, in the video summarization task, simply matching frames might overlook the subtle transitions that connect scenes, while in temporal reasoning tasks—such as answering *why does the woman need to drink water at the beginning of the video?*—it is crucial to concentrate on the beginning part of the video. These matching-based methods fail to account for these frame-to-frame interactions and the relative positional information essential for a comprehensive understanding of the video. To solve

054 these problems, we introduce an innovative approach named FRAME-VOYAGER that learns to query
055 the subset of frames in a combinational manner, rather than retrieving individual frames separately.
056 This capability is essential for understanding dynamic scenes and the global context of events.

057 To train FRAME-VOYAGER, we encounter two main challenges: **1) High Learning Complexity:**
058 Learning the optimal combination of frames poses a combinatorial optimization problem. For instance,
059 selecting 8 frames from a 128-frame video yields around 1.4×10^{12} possible frame combinations.
060 **2) Lack of Labeled Data:** There are currently no available datasets to facilitate the learning of such
061 combinatorial problems in videos. We must address the question of how to construct a training dataset
062 with minimal human effort. **To address the first challenge,** we formulate the combinatorial problem
063 as a ranking task. Specifically, we train the model to rank the given frame combinations (*i.e.*, subsets)
064 based on supervised ranking scores, which proves to be more efficient than forcing the model to
065 search the optimal frame combination in a huge search space (Cao et al., 2007). Assume that for each
066 frame combination, we have an annotation of ranking based on its usefulness in eventually generating
067 the correct answer (by addressing the second challenge). Given a batch of frame combinations, the
068 model learns to assign a higher reward to those with higher rankings. In other words, the model’s
069 objective is to maximize the reward for higher-ranked frame combinations. **To tackle the second**
070 **challenge,** we propose leveraging a pre-trained Video-LLM to generate a ranking score for each
071 frame combination, based on the prediction loss when the combination is input together with the
072 query into this Video-LLM. The intuition is that a more effective frame combination will result in
073 a lower prediction loss, indicating a higher likelihood of generating correct answers. Specifically,
074 assume the original video has M frames and the Video-LLM accepts only T frames for input. We
075 evaluate all frame combinations (*i.e.*, the total number is $\mathcal{C}(M, T)$) and rank them based on the
076 prediction losses provided by the Video-LLM. The frame combinations with lower losses rank
077 higher. These sorted frame combinations are then used for training FRAME-VOYAGER. Finally, the
078 trained FRAME-VOYAGER is used for choosing a frame combination to input into Video-LLMs for
downstream tasks.

079 To evaluate FRAME-VOYAGER, we plug it into two versions of the state-of-the-art Video-LLM named
080 VILA (VILA-8B and VILA-40B, Lin et al. (2024b)) and conduct experiments on four widely-used
081 Video Question Answering benchmarks, Video-MME (Fu et al., 2024a), MLVU (Zhou et al., 2024),
082 NextQA (Xiao et al., 2021) and ActivityNet-QA (Yu et al., 2019). Experiment results show that
083 using the frame combination “chosen” by FRAME-VOYAGER achieves significant performance im-
084 provements, compared to the conventional uniform sampling and text-frame retrieval (*i.e.*, individual
085 text-frame matching) methods, especially for the cases requiring reasoning and information synopsis
086 in long videos. **Our contributions** are thus two-fold: 1) We unveil the importance of combinational
087 frame selection for video understanding tasks and propose an efficient method FRAME-VOYAGER
088 that learns to do this frame selection automatically. The FRAME-VOYAGER itself is a plug-and-play
089 module that can be applied to different Video-LLM architectures; 2) We formulate and learn FRAME-
090 VOYAGER in a task of ranking frame combinations and introduce an automatic labeling pipeline to
091 generate training datasets.

093 2 RELATED WORK

094
095 Transformer-based LLMs have revolutionized the field of natural language processing, achieving
096 remarkable advancements by scaling up model sizes and expanding pre-training datasets (Brown
097 et al., 2020; OpenAI, 2023; Chowdhery et al., 2023; Touvron et al., 2023). Researchers further
098 extend LLMs into a multi-modality manner by fusing multi-modality information into the inputs
099 of LLMs (Zhang et al., 2024b; Liu et al., 2023). In this work, we focus on Video-LLMs, and we
100 consider the most widely-used structure (Lin et al., 2024b), where frames are adapted as visual tokens
101 and then temporally fed into LLMs alongside text tokens in an auto-regressive way.

102 However, in existing Video-LLM models, a single frame is typically represented by 64-256 visual
103 tokens (Liu et al., 2023; Lin et al., 2024b; Cheng et al., 2024). Due to the input limitations of LLMs,
104 the number of frames that can be processed by Video-LLM models is often constrained. Some studies
105 apply techniques for handling long LLM inputs to support more frames (Miao et al., 2023; Wan
106 et al., 2024; Xiong et al., 2024; Xue et al., 2024; Song et al., 2024), but this approach significantly
107 increases computational complexity and can lead to issues such as the “lost-in-the-middle” effect
and hallucinations (Liu et al., 2024c). Other studies, while keeping the frame input limit unchanged,

use alternative sampling strategies instead of the default uniform sampling to obtain higher-quality frames as inputs. Some initial attempts focus on identifying transition frames (Lu & Grauman, 2013; Rochan et al., 2018; Rochan & Wang, 2019) or using frame clustering (Liang et al., 2024; Han et al., 2024) to find central frames, but these methods often overlook the information from the query. Subsequent research view this problem as an individual text-frame (segment or cluster) matching task (Wang et al., 2024a; Yu et al., 2024; Wang et al., 2024b; 2025; 2024c), attempting to select frames that are semantically closest to the query. However, this method is still sub-optimal as it ignores frame-to-frame relationships, failing in complex video understanding tasks that require multi-frame or temporal information. An alternative way is to forcibly migrate the grounded video question answering (GVQA) methods (Xiao et al., 2024; Liu et al., 2025) to general video question answering. However, GVQA methods focus on identifying specific continuous temporal segments directly related to a question, which cannot meet the requirements of general video question answering.

Therefore, to the best of our knowledge, our method is the first to consider the combination of frames as a whole, aiming to find the optimal combination that can best answer the query under the constraint of frame length limitations.

3 FRAME-VOYAGER

In the research context of Video-LLMs, typical video-language tasks such as video understanding, summarization, and reasoning can be formulated as video question answering tasks. The input and output of Video-LLMs are thus in the format of (*video, query*) and *answer*, respectively. The *video* here is typically not the entire video but rather a subset of frames, *i.e.*, frame combination, due to the token length limitations. Our research question is thus how to get the “optimal” subset of frames in this *video* to answer the *text query* correctly. Our method is called FRAME-VOYAGER. To train it with manageable complexity, we downsample the entire video to a fixed number of M frames using uniform sampling. Then, we use FRAME-VOYAGER to evaluate T -frame combinations sampled from these M frames, where $M \gg T$. The training is supervised and the labeled data are generated by a pre-trained reference Video-LLM, as elaborated in Section 3.1.

Given that the optimal combination of frames must be identified in a huge search space, one may wonder: *How is FRAME-VOYAGER’s training supervised?* We answer this question by formulating the problem as a ranking task (for which it is easy to get labeled data, *i.e.*, the second challenge), rather than looking for “optimal” (as it is non-trivial to learn, *i.e.*, the first challenge). In the following subsections, we elaborate on this task by introducing the pipeline of ranking data collection (Section (3.1)) as well as the training and inference processes of FRAME-VOYAGER (Section (3.2)).

3.1 DATA COLLECTION

We propose a human-free data collection and annotation pipeline for frame combinations. The overall process is demonstrated in Figure 1.

Our pipeline is based on a simple intuition: *if one frame combination is better than another, it will produce a lower language modeling loss when used as input to any trained Video-LLM.* For each (*video, query*) pair, we evaluate all possible combinations of T frames selected from a total of M video frames, resulting in $\mathcal{C}(M, T)$ combinations, where $\mathcal{C}(M, T)$ is the binomial coefficient representing the number of ways to choose T items from M . Each combination, along with the *query*, is then input into a trained reference Video-LLM to calculate the combination loss, *i.e.*, language modeling loss against the ground-truth *answer*. We collect the loss values for each combination and rank them from best to worst by sorting the losses in ascending order. It is worth noting that as M increases, the potential number of combinations $\mathcal{C}(M, T)$ grows exponentially, making exhaustive traversal computationally infeasible. For example, when $M = 64$ and $T = 8$, the total number of combinations is approximately $\mathcal{C}(64, 8) \approx 4 \times 10^9$. Considering that the majority of the training data are with short videos, we use smaller combinations during training, such as $\mathcal{C}(16, 2)$ or $\mathcal{C}(32, 4)$. We observe from experiments that models trained with smaller combinations exhibit generalization capabilities when larger values of M and T are used during inference for longer video or complex reasoning. The specific choices of M and T employed in our experiments are detailed in Section 4.1.

To improve the ranking efficiency, we apply two filters for (*video, query*) pairs: we filter out 1) the pairs with an excessively high averaged loss, as these pairs may represent outlier cases or weak

162
163
164
165
166
167
168
169
170
171
172

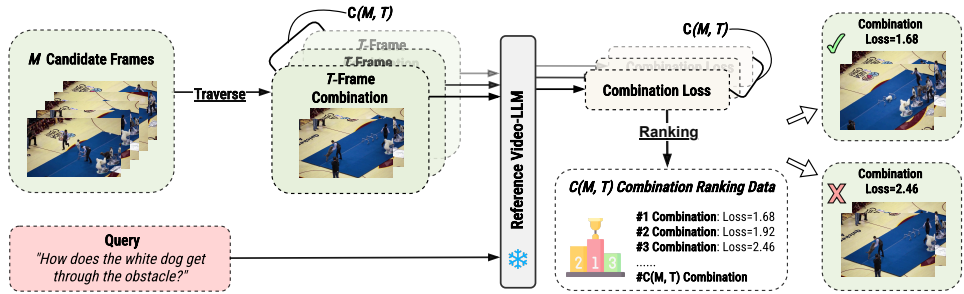


Figure 1: The data collection pipeline of FRAME-VOYAGER. Given a video of M frames, we traverse its T -frame combinations, feed them into a Video-LLM, and rank them based on the reference Video-LLM’s prediction losses. At last, we train FRAME-VOYAGER to query the frame combinations with lower losses. Please note that we omit filtering steps in this figure for clarity. $C(M, T)$ is the binomial coefficient representing the number of ways to choose T items from M .

173
174
175
176
177
178
179
180
181
182
183
184
185
186
187
188
189

video-query correlations; and 2) the pairs with low variance in the losses across their combinations, as these pairs are not sensitive to the quality of combinations, *e.g.*, the correct answer may be generated solely based on the Video-LLM’s inherent language prior without referring to any input content.

As a result, for each (*video, query*), we can obtain rankings for all $C(M, T)$ frame combinations, *i.e.*, the combination ranking data in Figure 1. Each item in combination ranking data contains the indices of frames within the combination and its corresponding rank. For instance, given $M = 8$ and $T = 2$, the combination $Comb = \langle \{Frame^2, Frame^5\}, \#6 \rangle$ means that it contains the 2-th and 5-th frames from M candidate frames, and it ranks at the $\#6$ position given all traversed $C(8, 2)$ combinations.

3.2 MODEL TRAINING AND INFERENCE

190
191
192
193
194

In this section, we elaborate on the training and inference details for FRAME-VOYAGER. Give a pre-trained Video-LLM, *e.g.*, VILA-8B (Lin et al., 2024b), we implement FRAME-VOYAGER as a lightweight plug-and-play module on it. For training this module, we use the M candidate frames and query as input to the model, and our FRAME-VOYAGER is thus learned to capture both query-frame and frame-to-frame relationships. The overall process is demonstrated in Figure 2.

195
196
197
198
199
200
201
202
203
204
205
206
207

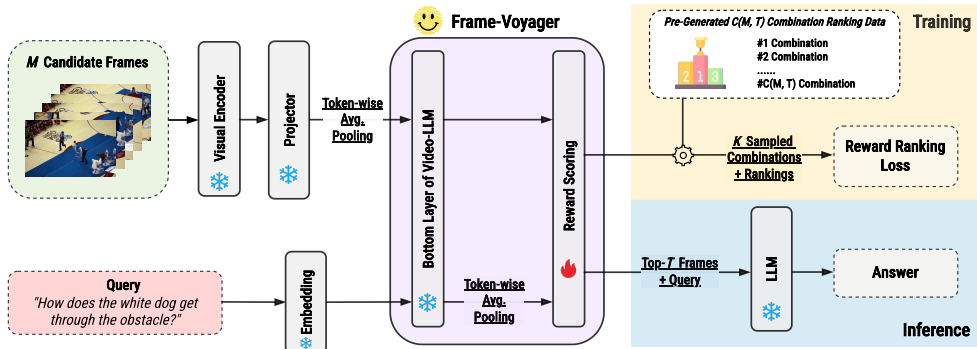


Figure 2: Training and inference processes of FRAME-VOYAGER. In the training, FRAME-VOYAGER is fed with all M candidate frames and learns to rank K sampled combinations from pre-generated combination ranking data in Section 3.1. Each combination contains T frames. As for the inference, FRAME-VOYAGER selects top- T frames with highest rewards to form the predicted frame combination. Note that there is no parameter to update during the inference.

213
214
215

Frame and Query Features. Given uniformly sampled M frames as candidate frames for each input (*video, query*) pair, we utilize the visual encoder followed by the Video-LLM projector to convert each frame into a sequence of visual tokens. Each visual token has the same size as the

word token embedding of the LLM backbone. Thus, for M frames, we have an initial feature map $\mathbf{X}' \in \mathbb{R}^{M \times N \times d}$, where M is the number of frames, N denotes the number of visual tokens per frame, and d represents the feature dimension. We further perform token-wise average pooling before feeding them into LLMs for computational efficiency, *i.e.*, averaging N visual tokens, on the initial frame feature map $\mathbf{X}' \in \mathbb{R}^{M \times N \times d}$ to obtain refined frame feature $\mathbf{X} \in \mathbb{R}^{M \times d}$. Concurrently, the query can be tokenized as Q tokens, and filled with word embeddings of the backbone LLM. The operation will produce $\mathbf{Y} \in \mathbb{R}^{Q \times d}$ for textual information.

Cross-Modality Interaction Modeling. To model both query-frame and frame-to-frame interactions, we leverage the bottom layers of LLMs. These transformer layers, which utilize the self-attention, are well pre-trained for vision-language tasks (Vaswani et al., 2017; Stan et al., 2024). Thus we concatenate the frame feature \mathbf{X} and query feature \mathbf{Y} , and feed them together into LLMs’ bottom layers. Importantly, all M candidate frames are processed simultaneously, rather than individually feeding T frames per combination, as FRAME-VOYAGER needs to model the entire set of M candidate frames to capture the relationships within frames. The generated cross-attentive multimodal features are denoted as $\mathbf{X}_{\text{BL}} \in \mathbb{R}^{M \times d}$ for frames and $\mathbf{Y}_{\text{BL}} \in \mathbb{R}^{Q \times d}$ for the query. The BL refers for “Bottom Layer”.

Frame Combination Reward. As mentioned, we formulate the combinatorial problem as a ranking task. Thus, for each frame combination, we need to compute its combination reward for further ranking-based training. First, we apply the token-wise average pooling on the cross-attentive multimodal features \mathbf{Y}_{BL} of query, and feed features into a feed-forward network (FFN). The generated final query feature is $\mathbf{Y}_{\text{FFN}} \in \mathbb{R}^h$, where h is the output dimension of the feed-forward network. The frame feature map \mathbf{X}_{BL} is also converted by another feed-forward network to get the final features $\mathbf{X}_{\text{FFN}} \in \mathbb{R}^{M \times h}$. Then we simply measure the reward for a given frame combination as the averaged reward of the frames within the combination as:

$$r(\text{Comb}) = \mathbb{E}_{i \in \text{Comb}}[r(\text{Frame}^i)]. \quad (1)$$

The reward for i -th frame (*i.e.*, i -th row in \mathbf{X}_{FFN}) with respect to the query and other frames, is computed as:

$$r(\text{Frame}^i) = \text{cosine}(\mathbf{Y}_{\text{FFN}}, \mathbf{X}_{\text{FFN}}^i). \quad (2)$$

Training. Inspired by the reward ranking loss function in (Ouyang et al., 2022), we train FRAME-VOYAGER via reward modeling to align its outputs with the optimal combination. To be specific, given the combination ranking data generated by the pipeline in Section 3.1, we uniformly sample K ranked combinations, with each combination consisting of T frames. Any two combinations sampled from the K frame combinations are selected to form a training pair ($\mathcal{C}(K, 2)$ training pairs in total), with the frame combination having a lower loss in each pair designated as the chosen sample and the one with a higher loss as the rejected sample. Overall, given K ranked combinations, the training objective, *i.e.*, reward ranking loss, is calculated as:

$$\mathcal{L} = -\frac{1}{\mathcal{C}(K, 2)} \mathbb{E} \left[\log \left(\delta(r(\text{Comb}_w) - r(\text{Comb}_l)) \right) \right], \quad (3)$$

where Comb_w denotes the preferred frame combination, and Comb_l represents the rejected one.

Inference. During inference, we plug the conventional Video-LLM models with our FRAME-VOYAGER module. Suppose that we uniformly sample M candidate frames and expect T frames as the visual input for Video-LLMs. The process remains consistent as the training procedure until the computation of the reward for frames. After that, we adopt the most efficient way to sample T frames, *i.e.*, selecting the top T frames with the highest rewards while maintaining their original temporal order in the video. The reason is that each reward of the frame here is optimized under combinational ranking supervision and incorporates the interaction information of the query and other frames.

4 EXPERIMENTS

4.1 EXPERIMENT SETTINGS

Backbone Models. We use three variants of the state-of-the-art Video-LLM called VILA (Lin et al., 2024b): VILA-8B, VILA-40B and LLaVA-One-Vision-7B. VILA-8B employs SigLIP (Zhai et al., 2023) as its visual encoder and Llama3-8B (Dubey et al., 2024) as its LLM backbone, while VILA-40B utilizes InternViT-6B (Chen et al., 2024) for visual encoding and Yi-34B (Young et al., 2024) as its LLM backbone.

Training Data. To ensure that FRAME-VOYAGER is trained on a diverse range of questions, we examine the video datasets used in VILA (Lin et al., 2024b) and LLaVA-OneVision (Li et al., 2024b). We select the training set of NextQA (Xiao et al., 2021) and VideoChatGPT (Maaz et al., 2024), on which we apply our proposed pipeline to create a training dataset for FRAME-VOYAGER. We empirically set the values of M and T based on the video length and question difficulty in these two datasets. Specifically, for NextQA, which features shorter videos and simpler questions, we select 16 candidate frames per video and explore all 120 possible 2-frame combinations. For VideoChatGPT, we select 32 candidate frames from each video and evaluate all 35,960 possible 4-frame combinations. During the filtering process, we exclude the $(video, query)$ pairs with an average loss larger than 7 and select pairs within the top 30% and 10% ranked by the variance of losses for the two datasets, respectively. After filtering, we obtain about 5,500 and 7,000 samples for these two datasets.

Benchmarks. We evaluate FRAME-VOYAGER on four widely-adopted video benchmarks: Video-MME (Fu et al., 2024a), MLVU (Zhou et al., 2024), NextQA (Xiao et al., 2021) and ActivityNet-QA (Yu et al., 2019). The former two evaluation datasets are tailored for long video assessments, while the latter two focus on short videos. We uniformly downsample the video to 128 candidate frames and each time select 8 frames to compose a frame combination. The LMMs-Eval Library (Li et al., 2024a) is used for evaluation, and accuracy is reported across all benchmarks. Note that we report the accuracy scores of Video-MME under both without (no sub.) and with (sub.) subtitles settings.

Implementation Details. During the FRAME-VOYAGER dataset construction, VILA-8B is consistently adopted as the reference Video-LLM for generating loss due to resource limitations. During training, we set $K = 4$ for sampling combination ranking data. VILA-8B is trained using DeepSpeed (Aminabadi et al., 2022) ZeRO2 with 8 H100 GPUs, while VILA-40B is trained using ZeRO3 setting with 32 H100 GPUs. The batch size (with accumulation) is set to 64 and the learning rate is $1e^{-3}$. The training of FRAME-VOYAGER is conducted over 40 epochs requiring approximately 8 hours for VILA-8B whereas over 20 epochs for VILA-40B, taking around 20 hours. All model inferences are performed on 8 H100 GPUs.

4.2 RESULTS AND ANALYSIS

Comparison with state-of-the-art methods. Table 1 presents the comparison of FRAME-VOYAGER with leading Video-LLMs, organized by the size of their backbone LLMs. For models with LLMs of

Table 1: Comparing Video-LLMs with and without FRAME-VOYAGER as an additional module. Except for ours (+FRAME-VOYAGER) and the models with *, all results are copied from the related papers of benchmarks or models. The two VILA baselines utilize uniform sampling. For the Video-MME benchmark, we report results under two standard settings: without subtitles (no sub.) and with subtitles (sub.). ANQA refers to ActivityNetQA. Accuracy sign % is omitted for clarity.

Model	LLM Size	Video-MME (no sub. / sub.)				MLVU	ANQA	NextQA
		Overall	Short	Medium	Long			
Video Length		17min	1.3min	9min	41min	12min	2min	0.8min
Video-LLaVA	7B	39.9 / 41.6	45.3 / 46.1	38.0 / 40.7	36.2 / 38.1	47.3	45.3	-
Qwen-VL-Chat	7B	41.1 / 41.9	46.9 / 47.3	38.7 / 40.4	37.8 / 37.9	-	-	-
ST-LLM	7B	37.9 / 42.3	45.7 / 48.4	36.8 / 41.4	31.3 / 36.9	-	50.9	-
VideoChat2	7B	39.5 / 43.8	48.3 / 52.8	37.0 / 39.4	33.2 / 39.2	44.5	49.1	-
Chat-UniVi-V1.5	7B	40.6 / 45.9	45.7 / 51.2	40.3 / 44.6	35.8 / 41.8	-	46.1	-
VideoLLaMA2	7B	47.9 / -	56.0 / -	45.4 / -	42.1 / -	-	49.9	-
LLaVA-NeXT-QW2	7B	49.5 / -	58.0 / -	47.0 / -	43.4 / -	-	-	-
LongVILA ^{128frm}	8B	49.2 / -	60.2 / -	48.2 / -	38.8 / -	-	-	-
LongVILA ^{256frm}	8B	50.5 / -	61.8 / -	49.7 / -	39.7 / -	-	-	-
VILA*	8B	47.5 / 50.0	57.8 / 61.6	44.3 / 46.2	40.3 / 42.1	46.3	53.7	55.6
+FRAME-VOYAGER	8B	50.5 / 53.6	60.3 / 65.0	47.3 / 50.3	43.9 / 45.3	49.8	55.7	60.8
LLaVA-One-Vision	7B	53.3 / -	64.0 / -	52.1 / -	43.8 / -	58.5	41.7	72.5
+FRAME-VOYAGER	7B	57.5 / -	67.3 / -	56.3 / -	48.9 / -	65.6	48.4	73.9
VideoLLaMA2	8×7B	47.9 / 49.7	- / -	- / -	- / -	-	50.3	-
VITA	8×7B	55.8 / 59.2	65.9 / 70.4	52.9 / 56.2	48.6 / 50.9	-	-	-
LLaVA-NeXT-Video	34B	52.0 / 54.9	61.7 / 65.1	50.1 / 52.2	44.3 / 47.2	-	58.8	-
VILA*	34B	58.3 / 61.6	67.9 / 70.7	56.4 / 59.8	50.4 / 52.1	57.8	56.8	62.9
+FRAME-VOYAGER	34B	60.0 / 63.8	70.3 / 73.1	58.3 / 62.7	51.2 / 55.7	61.1	57.9	67.3

Table 2: **RQ1.** Accuracies (%) for using different frame extraction methods on Video-MME (without subtitles). *Q*: whether query information is used. *Comb*: whether considering frame combination.

	<i>Q</i>	<i>Comb</i>	Video-MME
VILA-8B (Uniform)	✗	✗	47.5
+ RGB Histogram	✗	✗	45.9
+ Edges Change Ratio	✗	✗	47.3
+ Optical Flow	✗	✗	46.7
+ Katna	✗	✗	45.7
+ MDF	✗	✗	47.8
+ TempGQA	✓	✗	46.4
+ CLIP	✓	✗	48.5
+ SigLIP	✓	✗	48.3
+ InternViT-6B	✓	✗	49.1
+ SeViLA	✓	✗	49.3
+ VILA-Embedding	✓	✗	48.8
+ FRAME-VOYAGER	✓	✓	50.5

Table 3: **RQ2.** The ablation study (%) on different dataset collection methods. All results are evaluated on Video-MME (without subtitles). “Comb.”: frame combination.

	Video-MME
(1) NextQA	48.7
(2) VideoChatGPT w/ Filtering	49.1
(3) VideoChatGPT w/o Filtering	48.3
(4) All Data + Top-1 Rank Comb.	48.9
(5) All Data + $K=2$	49.4
(6) All Data + $K=8$	49.7
FRAME-VOYAGER ($K=4$)	50.5

8B parameters or fewer, we evaluate Video-LLaVA (Lin et al., 2024a), Qwen-VL-Chat (Bai et al., 2023), ST-LLM (Liu et al., 2024d), VideoChat2 (Li et al., 2023b), Chat-UniVi-V1.5 (Jin et al., 2024b), VideoLLaMA2 (Cheng et al., 2024), LLaVA-NeXT-QW2 (Liu et al., 2024b) and LongVILA (Xue et al., 2024). For larger models, we compare FRAME-VOYAGER with VideoLLaMA2 (Cheng et al., 2024), VITA (Fu et al., 2024b) and LLaVA-NeXT-Video (Zhang et al., 2024c).

Among the models with LLMs of 8B parameters or fewer, FRAME-VOYAGER achieves the best overall performance. On the Video-MME benchmark (without subtitles), it outperforms the vanilla VILA-8B by 3.0%, with a notable 3.6% gain on long videos. Remarkably, FRAME-VOYAGER, using only 8 frames as input into VILA, surpasses the VILA variant LongVILA, which utilizes 128 and 256

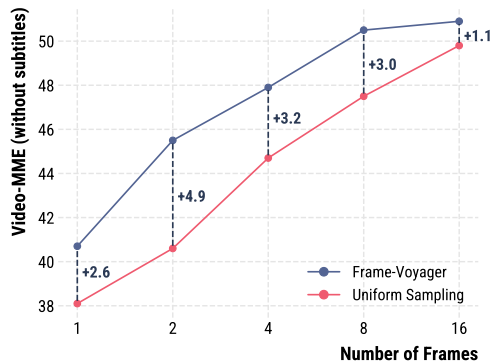


Figure 3: **RQ3.** Accuracies (%) of uniform sampling and FRAME-VOYAGER on Video-MME (without subtitles) regarding number of frames.

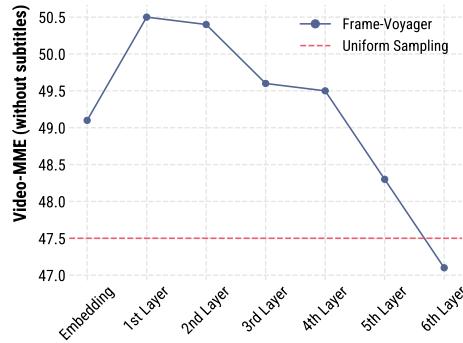


Figure 4: **RQ4.** Accuracies (%) of FRAME-VOYAGER reusing different layers of the LLM on Video-MME (without subtitles).

frames and requires additional training and system design. LongVILA improves its performance by inputting more frames, while FRAME-VOYAGER improves through querying more informative frame combinations, without changing the frame length limits of VILA. FRAME-VOYAGER outperforms LongVILA even on extremely long videos (average 41 minutes). This suggests that simply increasing the input number of frames may not always lead to better performance, since incorporating more frames might introduce noises and irrelevant information. More frames also reduce computing efficiency. Besides, among the larger Video-LLMs (with 8×7B and 34B LLM backbones), FRAME-VOYAGER consistently brings notable improvements over the vanilla VILA and other state-of-the-art models. These results highlight the importance of selecting and utilizing the optimal information from video for efficient video understanding. Last but not least, VILA-8B and VILA-40B employ distinct vision encoders and LLM backbones, as outlined in Section 4.1. Thus, the consistent performance improvements indicate that FRAME-VOYAGER functions as a plug-and-play module compatible with different Video-LLM architectures.

Research Question (RQ) 1: How does FRAME-VOYAGER compare to other frame extraction methods?

To evaluate the effectiveness of FRAME-VOYAGER on Video-LLMs, we conduct experiments with several baseline methods, all utilizing the same VILA-8B backbone, and the same number of frames for a fair comparison. We test rule-based shot boundary detection (SBD) methods, including Histogram (Sheena & Narayanan, 2015), Edges Change Ratio (Nasreen & Dr Shobha, 2013), Motion (Wolf, 1996), and MDF (Han et al., 2024), which select frames based on significant transitions in texture, structure, motion and inherent similarity. Frames with the most substantial changes are chosen as extracted frames. We also include Katna¹, a cluster-based method that extracts histograms from all frames and uses K-means clustering to select most representative frames near cluster centers. In addition, six frame-text matching methods (Liang et al., 2024; Wang et al., 2024a), VILA-Embedding, CLIP (Radford et al., 2021), SigLIP (Zhai et al., 2023), InternViT-6B (Chen et al., 2024), TempGQA (Xiao et al., 2024), and SeViLA (Yu et al., 2024) are employed to retrieve frames by calculating cosine similarity between query inputs and individual frames. Implementation details are presented in Appendix A.

Table 2 presents the comparison results on Video-MME (without subtitles). Rule-based methods perform worse than uniform frame sampling, likely due to inherent biases in these techniques. For instance, optical flow methods prioritize motion-heavy frames, while RGB histogram methods emphasize texture changes. These approaches overlook the input *query* and thus often fail to answer the *query*. Furthermore, although VILA Embedding and CLIP outperform uniform sampling, they still fall short compared to FRAME-VOYAGER. Their frame-by-frame extraction approach lacks a holistic understanding of the video, making them struggle with complex tasks requiring temporal reasoning and comprehensive video comprehension. Overall, the proposed FRAME-VOYAGER outperforms all the baselines, demonstrating superiority for frame subset selection and efficient video understanding.

¹<https://github.com/keplerlab/katna>

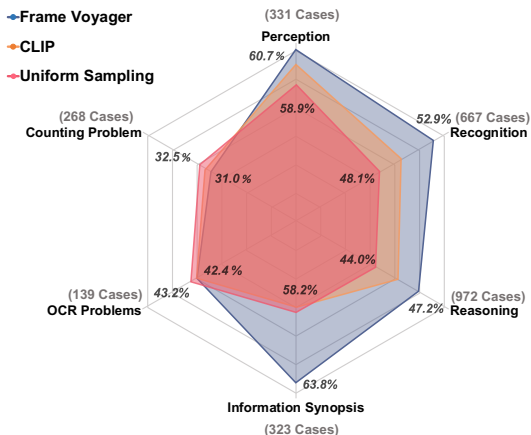


Figure 5: **RQ5.** Accuracies (%) of uniform sampling, CLIP, and FRAME-VOYAGER on six question types of the Video-MME. For each type, the maximum and minimum results are marked.

RQ3: How does the number of frames impact the performance of FRAME-VOYAGER?

In Figure 3, we demonstrate the performance of FRAME-VOYAGER on the Video-MME (without subtitles) by varying the number of chosen frames and comparing it to uniform sampling. Across different numbers of frames, FRAME-VOYAGER consistently outperforms uniform sampling. Notably, FRAME-VOYAGER achieves better results using only half the frames, *e.g.*, the 8-frame FRAME-VOYAGER surpasses the 16-frame uniform sampling. However, as the number of extracted frames increases, the performance gap between FRAME-VOYAGER and uniform sampling narrows. We think this is reasonable on the current public benchmarks which usually do not require a very large number of frames to answer the query. Using more frames may introduce unnecessary information, which could even limit performance gains.

RQ4: How does the design of FRAME-VOYAGER contribute to the performance?

FRAME-VOYAGER reuses the embedding layer and the first transformer layer of the backbone LLM. To validate this design choice, we assess the impact of reusing different components of the LLM, as presented in Figure 4. Reusing only the embedding layer’s bag-of-words features yields noticeable improvements. Incorporating one to two layers of the LLM enhances question understanding, leading to better performance. However, reusing additional layers results in a gradual performance decline. This decline occurs because the LLM remains frozen during FRAME-VOYAGER’s training, while lower-layer features are general-purpose, higher layers—with increased attention and fusion operations—shift the features towards language modeling, leading to diminished performance (Jin et al., 2024a).

RQ5: How does FRAME-VOYAGER perform on different types of questions?

Leveraging the question types defined in the Video-MME benchmark, we conduct a comparative analysis among three methods, *i.e.*, our FRAME-VOYAGER, the uniform sampling approach, the individual frame-query matching method based on CLIP, across six distinct categories of questions. The results are presented in Figure 5, where the maximum and minimum values are attached to each type in the figure. The results indicate that FRAME-VOYAGER achieves significant improvements in four of these categories, including an accuracy enhancement of 4.8% on the recognition task compared to uniform sampling. However, slight performance fluctuations are observed in the counting and OCR tasks. For instance, FRAME-VOYAGER results in one additional error in the counting problem compared to uniform sampling. We attribute these minor inconsistencies to VILA’s inherent limitations in effectively handling these specific types of tasks.

RQ2: What is the impact of each component on data collection?

To evaluate the effectiveness of each component in our dataset construction phase, we conduct a series of ablation studies summarized in Table 3. Specifically, we investigate the impact of individual datasets (1-2), analyze the role of data filtering (2-3), and explore the effects of different data usage strategies during training (4-6). In (4), we directly optimize the FRAME-VOYAGER by the combination ranked highest. In (5-6), we modify K , number of sampled combinations, during training. The results of (1-2) demonstrate additive performance gains from each dataset and the significant distribution differences between the two datasets enhance the query diversity. The results of (3) underscore the critical role of data filtering in eliminating instances unsuitable for training FRAME-VOYAGER. Experiments (4-6) provide some insights on data usage during training, revealing that varying the number of combinations can adversely affect reward computation. Moreover, results from (4) highlight the necessity of teaching FRAME-VOYAGER to discern better from worse combination via reward modeling, rather than merely training it to identify the combination.

We can also observe that, although CLIP-based method shows improvement over uniform sampling in the perception, recognition, and reasoning question types, they still fall short compared to FRAME-VOYAGER. In the information synopsis type, CLIP-based method performs even worse than uniform sampling. The reason is that CLIP-based methods ignore the global video information, whereas FRAME-VOYAGER explicitly models both the query-frame and frame-to-frame interactions.

RQ6: What does the combination extracted by FRAME-VOYAGER look like?

In Figure 9, we present one sampled case from Video-MME (Fu et al., 2024a). The *(video, query)* pair, with the query “*What is the small flying black dot at the start of the video*”, is evaluated across different methods. The frames obtained using uniform sampling provide limited information, with irrelevant background frames included. When using CLIP for frame-query matching, the retrieved frames show a small black dot in the first frame, followed by frames related to the terms “virus” and “protein”. However, these frames do not clarify what the small black dot represents.

In contrast, our model, FRAME-VOYAGER, effectively queries frame combinations by analyzing relationships between frames and modeling temporal information. This enables FRAME-VOYAGER to capture the critical details at the start of the video. The selected frame combinations reveal the trajectory of the “small black dot in flight”, ultimately identifying the “dot” as a “virus”. Additional case studies are provided in Appendix F.

5 CONCLUSIONS

In this work, we introduce FRAME-VOYAGER, a plug-and-play frame combination selection method that enhances Video-LLMs in video understanding tasks. We address the challenges of combination optimization by formulating it as a ranking task and implementing a ranking-based reward learning framework with a human-free data collection pipeline. Extensive experiments show that FRAME-VOYAGER not only significantly boosts the performance of baseline Video-LLMs like VILA, achieving state-of-the-art results, but also outperforms other frame selection methods. Comprehensive ablation studies further confirm its effectiveness. Overall, our work sets a strong baseline for Video-LLMs and guides future research on frame selection and optimization. As Video-LLMs evolve to tackle diverse tasks, our method offers an efficient solution to enhance broader video understanding.

LIMITATIONS

For the data construction, due to resource constraints, 1) we only generate the ranking data using VILA-8B, precluding experiments with more powerful Video-LLMs that might yield superior results. 2) The combinations for data construction are limited in size as the training set primarily focuses on short videos. Despite the promising improvements achieved, we highlight that applying FRAME-VOYAGER to longer videos with a greater number of frame combinations could potentially lead to further performance enhancements in processing extended video content. For the model framework, 1) we integrate our approach into existing Video-LLMs as a plug-in to ensure parameter efficiency, without additional fine-tuning of the backbone model. However, directly reusing the backbone’s parameters may not yield optimal results. Moreover, our simplified plug-in module could benefit from a more sophisticated design to further enhance overall performance. 2) Integrating our approach into the pre-training process of Video-LLMs remains unexplored, we hypothesize that learning frame combinations during pre-training could produce a more robust and effective model.

REFERENCES

- Reza Yazdani Aminabadi, Samyam Rajbhandari, Ammar Ahmad Awan, Cheng Li, Du Li, Elton Zheng, Olatunji Ruwase, Shaden Smith, Minjia Zhang, Jeff Rasley, and Yuxiong He. DeepSpeed-inference: enabling efficient inference of transformer models at unprecedented scale. In *Proceedings of the International Conference on High Performance Computing, Networking, Storage and Analysis (SC ’22)*, 2022.
- Jinze Bai, Shuai Bai, Shusheng Yang, Shijie Wang, Sinan Tan, Peng Wang, Junyang Lin, Chang Zhou, and Jingren Zhou. Qwen-vl: A frontier large vision-language model with versatile abilities. *arXiv:2308.12966*, 2023.

- 540 Tom Brown, Benjamin Mann, Nick Ryder, Melanie Subbiah, Jared D Kaplan, Prafulla Dhariwal,
541 Arvind Neelakantan, Pranav Shyam, Girish Sastry, Amanda Askell, Sandhini Agarwal, Ariel
542 Herbert-Voss, Gretchen Krueger, Tom Henighan, Rewon Child, Aditya Ramesh, Daniel Ziegler,
543 Jeffrey Wu, Clemens Winter, Chris Hesse, Mark Chen, Eric Sigler, Mateusz Litwin, Scott Gray,
544 Benjamin Chess, Jack Clark, Christopher Berner, Sam McCandlish, Alec Radford, Ilya Sutskever,
545 and Dario Amodei. Language models are few-shot learners. In *Proceedings of the 34th Annual
546 Conference on Neural Information Processing Systems (NeurIPS)*, pp. 1877–1901, 2020.
- 547 Zhe Cao, Tao Qin, Tie-Yan Liu, Ming-Feng Tsai, and Hang Li. Learning to rank: from pairwise
548 approach to listwise approach. In *Proceedings of the 24th International Conference on Machine
549 Learning (ICML)*, pp. 129–136, 2007.
- 550 Zhe Chen, Jiannan Wu, Wenhai Wang, Weijie Su, Guo Chen, Sen Xing, Muyan Zhong, Qinglong
551 Zhang, Xizhou Zhu, Lewei Lu, et al. Internvl: Scaling up vision foundation models and aligning
552 for generic visual-linguistic tasks. In *Proceedings of the 34th IEEE/CVF Conference on Computer
553 Vision and Pattern Recognition (CVPR)*, pp. 24185–24198, 2024.
- 554 Zesen Cheng, Sicong Leng, Hang Zhang, Yifei Xin, Xin Li, Guanzheng Chen, Yongxin Zhu, Wenqi
555 Zhang, Ziyang Luo, Deli Zhao, and Li Bing. Videollama 2: Advancing spatial-temporal modeling
556 and audio understanding in video-llms. *arXiv:2406.07476*, 2024.
- 557 Aakanksha Chowdhery, Sharan Narang, Jacob Devlin, Maarten Bosma, Gaurav Mishra, Adam
558 Roberts, Paul Barham, Hyung Won Chung, Charles Sutton, Sebastian Gehrmann, et al. Palm:
559 Scaling language modeling with pathways. *Journal of Machine Learning Research (JMLR)*, 24
560 (240):1–113, 2023.
- 561 Alexey Dosovitskiy, Lucas Beyer, Alexander Kolesnikov, Dirk Weissenborn, Xiaohua Zhai, Thomas
562 Unterthiner, Mostafa Dehghani, Matthias Minderer, Georg Heigold, Sylvain Gelly, Jakob Uszkoreit,
563 and Neil Houlsby. An image is worth 16x16 words: Transformers for image recognition at scale.
564 In *Proceedings of the 9th International Conference on Learning Representation (ICLR)*, 2021.
- 565 Abhimanyu Dubey, Abhinav Jauhri, Abhinav Pandey, Abhishek Kadian, Ahmad Al-Dahle, Aiesha
566 Letman, Akhil Mathur, Alan Schelten, Amy Yang, Angela Fan, et al. The llama 3 herd of models.
567 *arXiv:2407.21783*, 2024.
- 568 Chaoyou Fu, Yuhan Dai, Yondong Luo, Lei Li, Shuhuai Ren, Renrui Zhang, Zihan Wang, Chenyu
569 Zhou, Yunhang Shen, Mengdan Zhang, et al. Video-mme: The first-ever comprehensive evaluation
570 benchmark of multi-modal llms in video analysis. *arXiv:2405.21075*, 2024a.
- 571 Chaoyou Fu, Haojia Lin, Zuwei Long, Yunhang Shen, Meng Zhao, Yifan Zhang, Xiong Wang,
572 Di Yin, Long Ma, Xiawu Zheng, et al. Vita: Towards open-source interactive omni multimodal
573 llm. *arXiv:2408.05211*, 2024b.
- 574 Leo Gao, John Schulman, and Jacob Hilton. Scaling laws for reward model overoptimization. In
575 *Proceedings of the 40th International Conference on Machine Learning (ICML)*, pp. 10835–10866,
576 2023.
- 577 Wei Han, Hui Chen, Min-Yen Kan, and Soujanya Poria. Self-adaptive sampling for accurate video
578 question answering on image text models. In *Findings of the 2024 Annual Conference of the North
579 American Chapter of the Association for Computational Linguistics (Findings of NAACL 2024)*,
580 pp. 2522–2534, 2024.
- 581 Albert Qiaochu Jiang, Alexandre Sablayrolles, Arthur Mensch, Chris Bamford, Devendra Singh
582 Chaplot, Diego de Las Casas, Florian Bressand, Gianna Lengyel, Guillaume Lample, Lucile
583 Saulnier, L’elio Renard Lavaud, Marie-Anne Lachaux, Pierre Stock, Teven Le Scao, Thibaut Lavril,
584 Thomas Wang, Timothée Lacroix, and William El Sayed. Mistral 7b. *arXiv:2310.06825*, 2023.
- 585 Mingyu Jin, Qinkai Yu, Jingyuan Huang, Qingcheng Zeng, Zhenting Wang, Wenye Hua, Haiyan
586 Zhao, Kai Mei, Yanda Meng, Kaize Ding, Fan Yang, Mengnan Du, and Yongfeng Zhang.
587 Exploring concept depth: How large language models acquire knowledge at different layers?
588 *arXiv:2404.07066*, 2024a.
- 589
- 590
- 591
- 592
- 593

- 594 Peng Jin, Ryuichi Takano, Wancai Zhang, Xiaochun Cao, and Li Yuan. Chat-univi: Unified
595 visual representation empowers large language models with image and video understanding. In
596 *Proceedings of the 34th IEEE/CVF Conference on Computer Vision and Pattern Recognition*
597 *(CVPR)*, pp. 13700–13710, 2024b.
- 598
599 Bo Li, Peiyuan Zhang, Kaichen Zhang, Fanyi Pu, Xinrun Du, Yuhao Dong, Haotian Liu, Yuanhan
600 Zhang, Ge Zhang, Chunyuan Li, and Ziwei Liu. Lmms-eval: Accelerating the development of
601 large multimodal models, 2024a. URL <https://github.com/EvolvingLMMS-Lab/lmms-eval>.
- 602 Bo Li, Yuanhan Zhang, Dong Guo, Renrui Zhang, Feng Li, Hao Zhang, Kaichen Zhang, Yanwei
603 Li, Ziwei Liu, and Chunyuan Li. Llava-onevision: Easy visual task transfer. *arXiv:2408.03326*,
604 2024b.
- 605
606 Feng Li, Renrui Zhang, Hao Zhang, Yuanhan Zhang, Bo Li, Wei Li, Zejun Ma, and Chunyuan
607 Li. Llava-next-interleave: Tackling multi-image, video, and 3d in large multimodal models.
608 *arXiv:2407.07895*, 2024c.
- 609
610 Junnan Li, Dongxu Li, Silvio Savarese, and Steven Hoi. Blip-2: Bootstrapping language-image
611 pre-training with frozen image encoders and large language models. In *Proceedings of the 40th*
612 *International conference on machine learning (ICML)*, pp. 19730–19742, 2023a.
- 613 KunChang Li, Yinan He, Yi Wang, Yizhuo Li, Wenhai Wang, Ping Luo, Yali Wang, Limin Wang,
614 and Yu Qiao. Videochat: Chat-centric video understanding. *arXiv:2305.06355*, 2023b.
- 615
616 Hao Liang, Jiapeng Li, Tianyi Bai, Chong Chen, Conghui He, Bin Cui, and Wentao Zhang. Keyvide-
617 ollm: Towards large-scale video keyframe selection. *arXiv preprint arXiv:2407.03104*, 2024.
- 618
619 Bin Lin, Bin Zhu, Yang Ye, Munan Ning, Peng Jin, and Li Yuan. Video-llava: Learning united
620 visual representation by alignment before projection. In *Proceedings of the 2024 Conference on*
621 *Empirical Methods in Natural Language Processing (EMNLP)*, 2024a.
- 622 Ji Lin, Hongxu Yin, Wei Ping, Pavlo Molchanov, Mohammad Shoeybi, and Song Han. Vila: On
623 pre-training for visual language models. In *Proceedings of the 34th IEEE/CVF Conference on*
624 *Computer Vision and Pattern Recognition (CVPR)*, pp. 26689–26699, 2024b.
- 625
626 Haotian Liu, Chunyuan Li, Qingyang Wu, and Yong Jae Lee. Visual instruction tuning. In A. Oh,
627 T. Naumann, A. Globerson, K. Saenko, M. Hardt, and S. Levine (eds.), *Proceedings of the 37th*
628 *Annual Conference on Neural Information Processing Systems (NeurIPS)*, pp. 34892–34916, 2023.
- 629
630 Haotian Liu, Chunyuan Li, Yuheng Li, and Yong Jae Lee. Improved baselines with visual instruction
631 tuning. In *Proceedings of the 34th IEEE/CVF Conference on Computer Vision and Pattern*
632 *Recognition (CVPR)*, pp. 26296–26306, 2024a.
- 633
634 Haotian Liu, Chunyuan Li, Yuheng Li, Bo Li, Yuanhan Zhang, Sheng Shen, and Yong Jae Lee.
635 Llava-next: Improved reasoning, ocr, and world knowledge, 2024b. URL <https://llava-vl.github.io/blog/2024-01-30-llava-next/>.
- 636
637 Huabin Liu, Xiao Ma, Cheng Zhong, Yang Zhang, and Weiyao Lin. Timecraft: Navigate weakly-
638 supervised temporal grounded video question answering via bi-directional reasoning. In *European*
639 *Conference on Computer Vision*, pp. 92–107. Springer, 2025.
- 640
641 Nelson F. Liu, Kevin Lin, John Hewitt, Ashwin Paranjape, Michele Bevilacqua, Fabio Petroni, and
642 Percy Liang. Lost in the middle: How language models use long contexts. *Transactions of the*
643 *Association for Computational Linguistics (ACL)*, 12:157–173, 2024c.
- 644
645 Ruyang Liu, Chen Li, Haoran Tang, Yixiao Ge, Ying Shan, and Ge Li. St-llm: Large language
646 models are effective temporal learners. *arXiv:2404.00308*, 2024d.
- 647
648 Zheng Lu and Kristen Grauman. Story-driven summarization for egocentric video. In *Proceedings of*
649 *the 23rd IEEE Conference on Computer Vision and Pattern Recognition (CVPR)*, pp. 2714–2721,
650 2013.

- 648 Muhammad Maaz, Hanoona Rasheed, Salman Khan, and Fahad Shahbaz Khan. Video-chatgpt:
649 Towards detailed video understanding via large vision and language models. In *Proceedings of the*
650 *62nd Annual Meeting of the Association for Computational Linguistics (ACL)*, 2024.
- 651 Xupeng Miao, Gabriele Oliaro, Zhihao Zhang, Xinhao Cheng, Hongyi Jin, Tianqi Chen, and Zhihao
652 Jia. Towards efficient generative large language model serving: A survey from algorithms to
653 systems. *arXiv:2312.15234*, 2023.
- 654 Azra Nasreen and G Dr Shobha. Key frame extraction using edge change ratio for shot segmentation.
655 *International Journal of Advanced Research in Computer and Communication Engineering*, 2(11):
656 4421–4423, 2013.
- 657 OpenAI. Chatgpt: Optimizing language models for dialogue, 2023. URL [https://openai.com/
658 blog/chatgpt](https://openai.com/blog/chatgpt).
- 659 Long Ouyang, Jeffrey Wu, Xu Jiang, Diogo Almeida, Carroll Wainwright, Pamela Mishkin, Chong
660 Zhang, Sandhini Agarwal, Katarina Slama, Alex Ray, John Schulman, Jacob Hilton, Fraser Kelton,
661 Luke Miller, Maddie Simens, Amanda Askell, Peter Welinder, Paul F Christiano, Jan Leike,
662 and Ryan Lowe. Training language models to follow instructions with human feedback. In
663 *Proceedings of the 36th Annual Conference on Neural Information Processing Systems (NeurIPS)*,
664 pp. 27730–27744, 2022.
- 665 Alec Radford, Jong Wook Kim, Chris Hallacy, Aditya Ramesh, Gabriel Goh, Sandhini Agarwal,
666 Girish Sastry, Amanda Askell, Pamela Mishkin, Jack Clark, Gretchen Krueger, and Ilya Sutskever.
667 Learning transferable visual models from natural language supervision. In *Proceedings of the 38th*
668 *International Conference on Machine Learning (ICML)*, pp. 8748–8763, 2021.
- 669 Mrigank Rochan and Yang Wang. Video summarization by learning from unpaired data. In *Proceed-*
670 *ings of the 29th IEEE/CVF Conference on Computer Vision and Pattern Recognition (CVPR)*, pp.
671 7902–7911, 2019.
- 672 Mrigank Rochan, Linwei Ye, and Yang Wang. Video summarization using fully convolutional
673 sequence networks. In *Proceedings of the European Conference on Computer Vision (ECCV)*, pp.
674 347–363, 2018.
- 675 C Va Sheena and NK Narayanan. Key-frame extraction by analysis of histograms of video frames
676 using statistical methods. *Procedia Computer Science*, 70:36–40, 2015.
- 677 Enxin Song, Wenhao Chai, Guan hong Wang, Yucheng Zhang, Haoyang Zhou, Feiyang Wu, Haozhe
678 Chi, Xun Guo, Tian Ye, Yanting Zhang, et al. Moviechat: From dense token to sparse memory for
679 long video understanding. In *Proceedings of the 34th IEEE/CVF Conference on Computer Vision*
680 *and Pattern Recognition (CVPR)*, pp. 18221–18232, 2024.
- 681 Gabriela Ben Melech Stan, Raanan Yehezkel Rohekar, Yaniv Gurwicz, Matthew Lyle Olson, Anahita
682 Bhiwandiwalla, Estelle Aflalo, Chenfei Wu, Nan Duan, Shao-Yen Tseng, and Vasudev Lal. Lvlm-
683 intepret: An interpretability tool for large vision-language models. *arXiv:2404.03118*, 2024.
- 684 Nisan Stiennon, Long Ouyang, Jeffrey Wu, Daniel Ziegler, Ryan Lowe, Chelsea Voss, Alec Radford,
685 Dario Amodei, and Paul F Christiano. Learning to summarize with human feedback. In *Proceedings*
686 *of the 34th Annual Conference on Neural Information Processing Systems (NeurIPS)*, pp. 3008–
687 3021, 2020.
- 688 Hugo Touvron, Thibaut Lavril, Gautier Izacard, Xavier Martinet, Marie-Anne Lachaux, Timothée
689 Lacroix, Baptiste Rozière, Naman Goyal, Eric Hambro, Faisal Azhar, et al. Llama: Open and
690 efficient foundation language models. *arXiv:2302.13971*, 2023.
- 691 Ashish Vaswani, Noam Shazeer, Niki Parmar, Jakob Uszkoreit, Llion Jones, Aidan N Gomez, Ł ukasz
692 Kaiser, and Illia Polosukhin. Attention is all you need. In *Proceedings of the 31st Annual*
693 *Conference on Neural Information Processing Systems (NeurIPS)*, 2017.
- 694 Zhongwei Wan, Xin Wang, Che Liu, Samiul Alam, Yu Zheng, Zhongnan Qu, Shen Yan, Yi Zhu,
695 Quanlu Zhang, Mosharaf Chowdhury, et al. Efficient large language models: A survey. *Transac-*
696 *tions on Machine Learning Research (TMLR)*, 2024.

- 702 Haibo Wang, Chenghang Lai, Yixuan Sun, and Weifeng Ge. Weakly supervised gaussian contrastive
703 grounding with large multimodal models for video question answering. In *Proceedings of the 32nd*
704 *ACM Multimedia Conference (MM)*, 2024a.
- 705
706 Xiaohan Wang, Yuhui Zhang, Orr Zohar, and Serena Yeung-Levy. Videoagent: Long-form video
707 understanding with large language model as agent. In *European Conference on Computer Vision*,
708 pp. 58–76. Springer, 2025.
- 709
710 Xijun Wang, Junbang Liang, Chun-Kai Wang, Kenan Deng, Yu Lou, Ming C Lin, and Shan Yang.
711 Vila: Efficient video-language alignment for video question answering. In *European Conference*
712 *on Computer Vision*, pp. 186–204, 2024b.
- 713
714 Ziyang Wang, Shoubin Yu, Elias Stengel-Eskin, Jaehong Yoon, Feng Cheng, Gedas Bertasius, and
715 Mohit Bansal. Videotree: Adaptive tree-based video representation for llm reasoning on long
716 videos. *arXiv preprint arXiv:2405.19209*, 2024c.
- 717
718 Wayne Wolf. Key frame selection by motion analysis. In *Proceedings of the 1996 IEEE International*
719 *Conference on Acoustics, Speech, and Signal Processing Conference*, pp. 1228–1231, 1996.
- 720
721 Junbin Xiao, Xindi Shang, Angela Yao, and Tat-Seng Chua. Next-qa: Next phase of question-
722 answering to explaining temporal actions. In *Proceedings of the 31st IEEE/CVF Conference on*
723 *Computer Vision and Pattern Recognition (CVPR)*, pp. 9777–9786, 2021.
- 724
725 Junbin Xiao, Angela Yao, Yicong Li, and Tat-Seng Chua. Can i trust your answer? visually grounded
726 video question answering. In *Proceedings of the IEEE/CVF Conference on Computer Vision and*
727 *Pattern Recognition*, pp. 13204–13214, 2024.
- 728
729 Wenhan Xiong, Jingyu Liu, Igor Molybog, Hejia Zhang, Prajjwal Bhargava, Rui Hou, Louis Martin,
730 Rashi Rungta, Karthik Abinav Sankararaman, Barlas Oguz, et al. Effective long-context scaling
731 of foundation models. In *Proceedings of the 2024 Conference of the North American Chapter*
732 *of the Association for Computational Linguistics: Human Language Technologies (NAACL)*, pp.
733 4643–4663, 2024.
- 734
735 Fuzhao Xue, Yukang Chen, Dacheng Li, Qinghao Hu, Ligeng Zhu, Xiuyu Li, Yunhao Fang, Haotian
736 Tang, Shang Yang, Zhijian Liu, et al. Longvila: Scaling long-context visual language models for
737 long videos. *arXiv:2408.10188*, 2024.
- 738
739 An Yang, Baosong Yang, Binyuan Hui, Bo Zheng, Bowen Yu, Chang Zhou, Chengpeng Li,
740 Chengyuan Li, Dayiheng Liu, Fei Huang, Guanting Dong, Haoran Wei, Huan Lin, Jialong Tang,
741 Jialin Wang, Jian Yang, Jianhong Tu, Jianwei Zhang, Jianxin Ma, Jin Xu, Jingren Zhou, Jinze Bai,
742 Jinzheng He, Junyang Lin, Kai Dang, Keming Lu, Ke-Yang Chen, Kexin Yang, Mei Li, Min Xue,
743 Na Ni, Pei Zhang, Peng Wang, Ru Peng, Rui Men, Ruize Gao, Runji Lin, Shijie Wang, Shuai Bai,
744 Sinan Tan, Tianhang Zhu, Tianhao Li, Tianyu Liu, Wenbin Ge, Xiaodong Deng, Xiaohuan Zhou,
745 Xingzhang Ren, Xinyu Zhang, Xipin Wei, Xuancheng Ren, Yang Fan, Yang Yao, Yichang Zhang,
746 Yunyang Wan, Yunfei Chu, Zeyu Cui, Zhenru Zhang, and Zhi-Wei Fan. Qwen2 technical report.
747 *arXiv:2407.10671*, 2024.
- 748
749 Alex Young, Bei Chen, Chao Li, Chengen Huang, Ge Zhang, Guanwei Zhang, Heng Li, Jiangcheng
750 Zhu, Jianqun Chen, Jing Chang, et al. Yi: Open foundation models by 01. ai. *arXiv:2403.04652*,
751 2024.
- 752
753 Shoubin Yu, Jaemin Cho, Prateek Yadav, and Mohit Bansal. Self-chained image-language model for
754 video localization and question answering. *Proceedings of the 38th Annual Conference on Neural*
755 *Information Processing Systems (NeurIPS)*, 36, 2024.
- 756
757 Zhou Yu, Dejing Xu, Jun Yu, Ting Yu, Zhou Zhao, Yueting Zhuang, and Dacheng Tao. Activitynet-qa:
758 A dataset for understanding complex web videos via question answering. In *Proceedings of the*
759 *33rd AAAI Conference on Artificial Intelligence (AAAI)*, pp. 9127–9134, 2019.
- 760
761 Xiaohua Zhai, Basil Mustafa, Alexander Kolesnikov, and Lucas Beyer. Sigmoid loss for language
762 image pre-training. In *Proceedings of the IEEE/CVF International Conference on Computer Vision*
763 *(ICCV)*, pp. 11975–11986, 2023.

756 Hang Zhang, Xin Li, and Lidong Bing. Video-LLaMA: An instruction-tuned audio-visual language
757 model for video understanding. In *Proceedings of the 2023 Conference on Empirical Methods in*
758 *Natural Language Processing (EMNLP)*, pp. 543–553, 2023.

759 Peiyuan Zhang, Kaichen Zhang, Bo Li, Guangtao Zeng, Jingkang Yang, Yuanhan Zhang, Ziyue
760 Wang, Haoran Tan, Chunyuan Li, and Ziwei Liu. Long context transfer from language to vision.
761 *arXiv:2406.16852*, 2024a.

762 Renrui Zhang, Jiaming Han, Chris Liu, Peng Gao, Aojun Zhou, Xiangfei Hu, Shilin Yan, Pan Lu,
763 Hongsheng Li, and Yu Qiao. Llama-adapter: Efficient fine-tuning of language models with zero-init
764 attention. In *Proceedings of the 12th International Conference on Learning Representation (ICLR)*,
765 2024b.

766 Yuanhan Zhang, Bo Li, haotian Liu, Yong jae Lee, Liangke Gui, Di Fu, Jiashi Feng, Ziwei Liu,
767 and Chunyuan Li. Llava-next: A strong zero-shot video understanding model, 2024c. URL
768 <https://llava-vl.github.io/blog/2024-04-30-llava-next-video/>.

769 Junjie Zhou, Yan Shu, Bo Zhao, Boya Wu, Shitao Xiao, Xi Yang, Yongping Xiong, Bo Zhang,
770 Tiejun Huang, and Zheng Liu. Mlvu: A comprehensive benchmark for multi-task long video
771 understanding. *arXiv:2406.04264*, 2024.

772
773
774
775
776
777
778
779
780
781
782
783
784
785
786
787
788
789
790
791
792
793
794
795
796
797
798
799
800
801
802
803
804
805
806
807
808
809

A IMPLEMENTATION DETAILS OF FRAME EXTRACTION BASELINES IN RQ1

In executing the SBD methods, we utilize the OpenCV² library. We generate the disparity between each frame and its adjacent frame, utilizing both the difference of the RGB Histogram and Canny, as well as the optical flows. This process aids us in picking out T frames with the top- T greatest disparity values.

For the cluster-based approach, Katna, we directly use Katna API. It initially segments the videos according to content specifics and extracts a list of keyframes from each individual segment, employing the Histogram with K-means technique. Afterward, all segmented keyframe lists are merged to pick out the final T frames.

For VILA-Embedding, we utilize the visual feature after the projector and the text feature from word embedding to measure the cosine similarity after the average pooling. The cosine similarity is then used for ranking the frames. For CLIP, we use the hosted model on HuggingFace³ and directly rank and select top- T candidate frames according to their output logits.

B QUESTION TYPE ANALYSIS OF THE GENERATED DATASETS

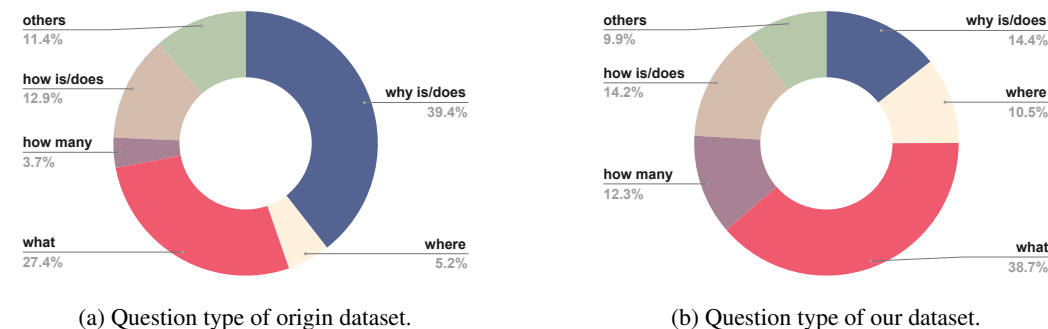


Figure 6: The question type distribution on NextQA dataset. Best viewed in color.

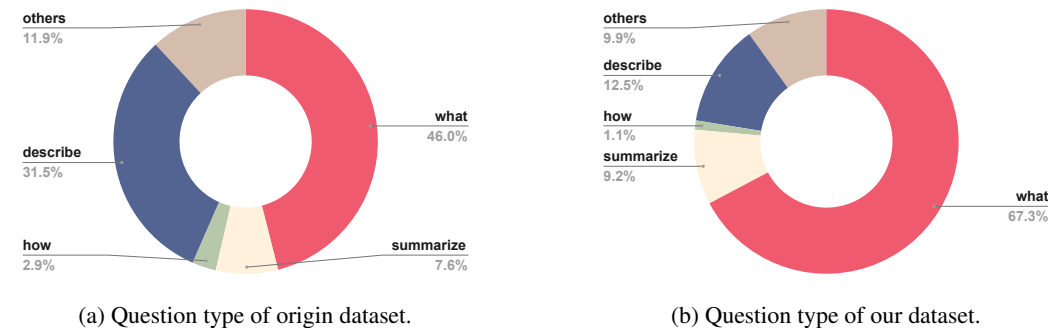


Figure 7: The question type distribution on VideoChatGPT dataset. Best viewed in color.

We observe similar patterns in Figure 6 and Figure 7. Taking the NextQA dataset as an example, the proportion of “what” type questions in the original dataset is 27.4%, whereas in our generated dataset, this proportion increases to 38.7%. Conversely, the proportion of “why is/does” type questions significantly decreases from 39.4% in the original dataset to 11.4% in our generated dataset.

The reason is that answers to questions starting with “what” tend to be shorter compared to those starting with “why is/does”. When we calculate the loss for each subset combination using Video-LLM, the auto-regressive loss for each token in the answer is computed based on all preceding tokens.

²<https://github.com/opencv/opencv>

³https://huggingface.co/docs/transformers/model_doc/clip

In the case of a long answer, the LLM’s prior knowledge may diminish the impact of the subset combination (as the LLM can predict subsequent tokens based on the earlier ones in the answer). This leads to more “why” cases being removed during our filtering process.

C ANALYSIS OF COMPUTATION COST

In this section, we analyze the additional overhead introduced by FRAME-VOYAGER based on VILA-8B. First, in terms of parameter size, our method introduces two MLPs, and the additional parameters account for 0.2% of the original model’s parameter. Next, we analyze the time overhead. During training, the original model required 5.1k GPU hours(Lin et al., 2024b), while FRAME-VOYAGER requires 64 GPU hours, representing an additional training time of 1.25% of the original.

For inference, we randomly sample 100 examples from Video-MME to measure the model’s inference latency. Using the experimental setting from our main paper, the average inference latency for the uniform sampling baseline is 1.329 seconds per example, while for FRAME-VOYAGER it is 1.696 seconds, indicating that our method introduces an additional latency overhead of approximately 27.6%.

Table 4: The ablation results on different number of candidate frames. For all experiments, we expand the candidate frames from 8 to 256, while freeze the number of chosen frames as 8. Results are reported on Video-MME dataset (without subtitles).

#candidate frames	8	16	32	64	128	256
Video-MME (%)	47.5	48.2	48.6	49.7	50.5	50.8

D A STUDY ON THE NUMBER OF CANDIDATE FRAMES

Table 5: The ablation results on different number of candidate frames. For all experiments, we expand the candidate frames from 8 to 256, while freeze the number of chosen frames as 8. Results are reported on Video-MME dataset (without subtitles).

#candidate frames	8	16	32	64	128	256
Video-MME (%)	47.5	48.2	48.6	49.7	50.5	50.8

As the number of candidate frames increases, more video information is captured within the selection pool. While selecting 8 frames from a larger candidate set, our method consistently improves results on the Video-MME dataset. As shown in Table 5, selecting 8 frames from a candidate pool of 128 frames yields a 3% improvement compared to selecting from just 8 frames (*i.e.*, uniform sampling). However, as the candidate set size increases further (from 128 to 256), the additional information brought by the expanded set becomes limited.

E CASE STUDY ON TRAINING DATA

To evaluate the training objective of our FRAME-VOYAGER, we examine random samples from the NextQA dataset after processing it through our data collection pipeline in Section 3.1. Figure 8 shows these sample cases, revealing a clear pattern: question-answer pairs with lower loss values show stronger alignment with the visual content. This correlation demonstrates that our loss-based ranking effectively identifies the most contextually relevant frames for answering questions. However, in cases with higher loss values, while the frames may contain relevant objects, they often lack sufficient visual information to fully answer the given questions.

918
919
920
921
922
923
924
925
926
927
928
929
930
931
932
933
934
935
936
937
938
939
940
941
942
943
944
945
946
947
948
949
950
951
952
953
954
955
956
957
958
959
960
961
962
963
964
965
966
967
968
969
970
971

1 *Question: How does the white dog get through the obstacle?*
Answer: Move under the obstacle

Higher Ranking with Loss=1.68 Lower Ranking with Loss=2.46

2 *Question: How many animals are involved in the video?*
Answer: two

Higher Ranking with Loss=2.89 Lower Ranking with Loss=4.08

3 *Question: Why did the boy in black extend his arm towards the baby near the end of the video?*
Answer: wants to feed baby

Higher Ranking with Loss=2.93 Lower Ranking with Loss=3.98

4 *Question: What is the attraction that they are taking photographs of?*
Answer: fjords

Higher Ranking with Loss=3.09 Lower Ranking with Loss=4.00

5 *Question: What does the short hair girl do after getting something from the top of the piano at the start?*
Answer: put it on her head

Higher Ranking with Loss=2.67 Lower Ranking with Loss=3.59

Figure 8: Case study from processed NextQA training data: These random samples show that lower loss values correlate with better visual-question alignment. The loss signal can enable learning to effectively select frame combinations for answering questions.

F CASE STUDY ON FRAME COMBINATIONS BY FRAME-VOYAGER

In Figure 10 and 11, we present additional case studies to highlight the effectiveness of our model. In Figure 10, the uniform sampling fails to capture key objects mentioned in the query. Similarly, the CLIP-based method struggles due to its limited OCR capabilities on special fonts, often match objects like “blue food dye”. In contrast, our FRAME-VOYAGER, accurately identifies the used ingredients in this video, providing sufficient video context to answer the query about which ingredients are not used.

Figure 11 further demonstrates the limitations of uniform sampling, which produces a lot of irrelevant background frames. While the CLIP-based method focuses on isolated keywords like “basketball” and “boy”, it lacks the ability to connect frames meaningfully. Our method, however, selects represen-

Question: Which object is depicted as a small flying black dot at the start of the video?
 A. Dust mites in the lungs. B. Virus.
 C. Protein Receptors. D. Black bacteria.
Answer: Virus.

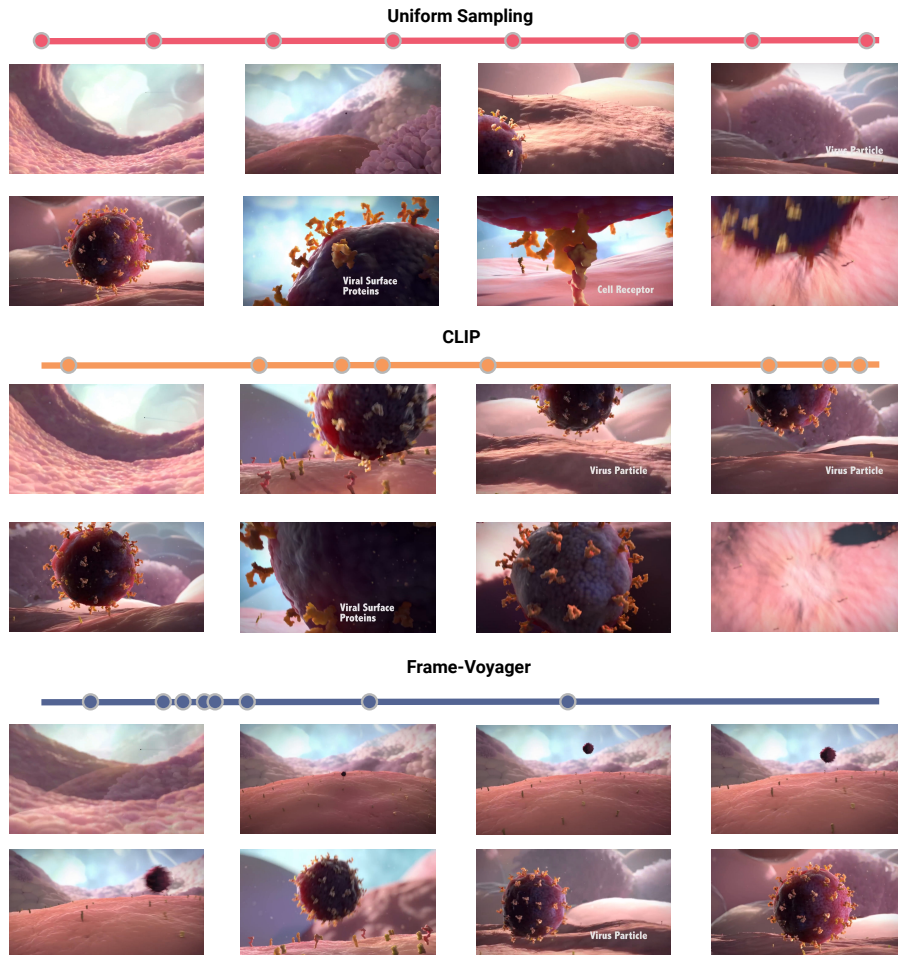


Figure 9: Case study from Video-MME: The horizontal lines represent the timeline, with points marking the time positions of frames extracted by different methods. Uniform sampling captures only a limited number of frames relevant to the query. While CLIP extracts more relevant frames, it struggles to capture the temporal dynamics of gradual zoom-in transitions. In contrast, FRAME-VOYAGER effectively selects a combination of frames that are both highly relevant to the query and accurately reflect the correct temporal sequence.

1026 tative frames based on the query, illustrating key events in temporal order—from the boy’s training to
1027 the basketball match, and finally, the podium.
1028
1029
1030
1031
1032
1033
1034
1035
1036
1037
1038
1039
1040
1041
1042
1043
1044
1045
1046
1047
1048
1049
1050
1051
1052
1053
1054
1055
1056
1057
1058
1059
1060
1061
1062
1063
1064
1065
1066
1067
1068
1069
1070
1071
1072
1073
1074
1075
1076
1077
1078
1079

1080
1081
1082
1083
1084
1085
1086
1087
1088
1089
1090
1091
1092
1093
1094
1095
1096
1097
1098
1099
1100
1101
1102
1103
1104
1105
1106
1107
1108
1109
1110
1111
1112
1113
1114
1115
1116
1117
1118
1119
1120
1121
1122
1123
1124
1125
1126
1127
1128
1129
1130
1131
1132
1133

Question: According to the video, which of the following ingredients is not used in the artwork?
 A. Shell B. Glue C. Blue Food Dye D. Oil

Answer: Shell

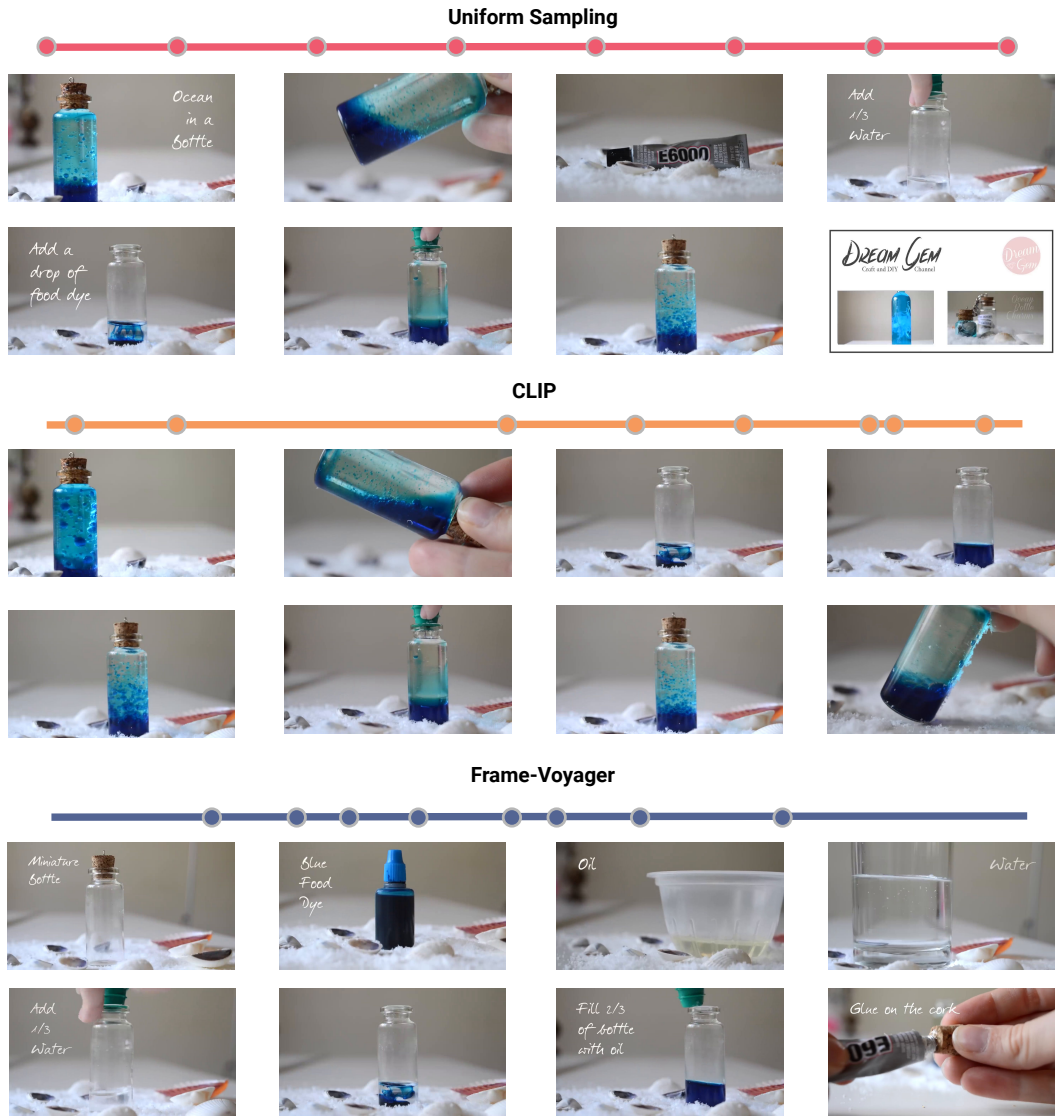


Figure 10: Case study from Video-MME: The horizontal lines represent the timeline, with points marking the time positions of frames extracted by different methods. We can see that the uniform sampling fails to capture key objects relevant to the query, while the CLIP-based method, due to its limited OCR capabilities on special fonts, incorrectly matches terms like “blue food dye”. In contrast, FRAME-VOYAGER effectively identifies the used ingredients, providing the necessary context to accurately answer the query about which ingredient is not used.

1134
1135
1136
1137
1138
1139
1140
1141
1142
1143
1144
1145
1146
1147
1148
1149
1150
1151
1152
1153
1154
1155
1156
1157
1158
1159
1160
1161
1162
1163
1164
1165
1166
1167
1168
1169
1170
1171
1172
1173
1174
1175
1176
1177
1178
1179
1180
1181
1182
1183
1184
1185
1186
1187

Question: What story does the video tell?
 A. A boy's basketball growing-up story B. Development of basketball
 C. How does NBA draft D. How do boys practice basketball

Answer: A boy's basketball growing-up story

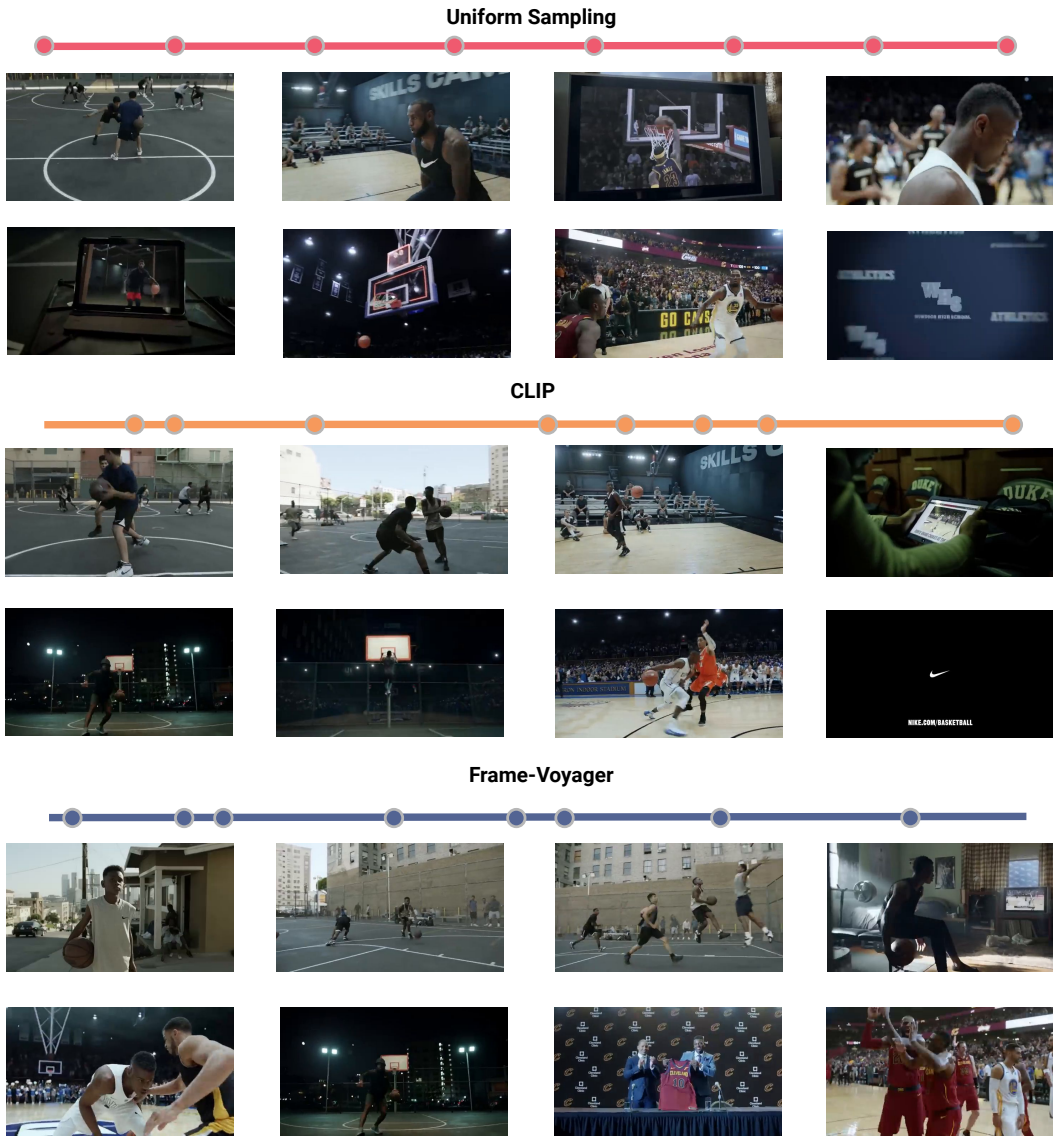


Figure 11: Case study from Video-MME: The horizontal lines represent the timeline, with points marking the time positions of frames extracted by different methods. It shows that uniform sampling produces a sequence containing many irrelevant background frames. The CLIP-based method, though focused on keywords like “basketball” and “boy”, fails to capture the temporal relationships between frames. Our approach can select high-quality frames that align with the query, illustrating key events in temporal order—from “boy’s training” to the “basketball match” and finally the “podium”.